A Dual-Band Implantable Antenna for Mobile Systems

Ansam Qasim Kamil
Middle Technical University, Baghdad, Iraq
ansamQasim@mtu.edu.iq

Received: 18 September 2024 | Revised: 10 October 2024 and 2 November 2024 | Accepted: 15 January 2025

 DOI: https://doi.org/10.48084/etasr.9035

ABSTRACT

In this paper, a miniaturized dual-band implantable antenna is presented for mobile communication services, as well as industrial and scientific applications. The proposed antenna, with compact dimensions of 37 × 35 × 1.6 mm³, operates efficiently at dual frequencies of 3.7 GHz and 6.2 GHz. It features a circular metal patch with rectangular-shaped slots, enabling stable radiation patterns, broadband impedance matching, and robust performance. The antenna achieves a gain of 3.47 dBi, a directivity of 4.5, and an efficiency of 86%, making it well-suited for 5G technology and other high-frequency applications. Compared to existing designs, the proposed antenna demonstrates significant improvements in efficiency and bandwidth while maintaining a compact size. These antennas are essential for handling the increased data demands and diverse frequency requirements of modern mobile systems. Future trends in wireless communication are rapidly evolving, addressing challenges, such as interference reduction, increased data demands, and enhanced network performance. The proposed antenna, with its high efficiency and compact design, aligns with these trends and is well-positioned to meet the requirements of the next-generation communication systems.

Keywords-dual-band; wideband; mobile system; circular; metal patch

I. INTRODUCTION

Dual-band antennas are essential for evolving mobile technologies, including 3G, 4G, and 5G systems. These antennas facilitate communication over multiple frequency bands, such as the S-band (2-4 GHz) and the C-band (4-8 GHz), by leveraging advanced design techniques. Key methods, such as slot-coupled patches, enhance bandwidth and reduce surface wave losses, enabling multiple resonant frequencies and broader operational bandwidths. To achieve efficient power transmission and minimize signal reflections, dual-band antennas require careful parameter optimization to balance performance, ensure stable radiation patterns, maintain high efficiency, and meet specific gain requirements. These designs must cater to various use cases and performance needs, particularly as multi-band and broadband antennas become integral to modern 3G, 4G, and 5G systems. A common approach to dual-band performance is combining multiple resonant elements or employing tuning techniques to achieve resonance at distinct frequencies [1]. Techniques, such as aperture coupling and impedance matching, further refine performance, allowing antennas to effectively operate in both the S-band and C-band [2]. For example, the 6.2 GHz band is used in radar systems, automotive collision avoidance, adaptive cruise control, and certain satellite communication and scientific applications, including radio astronomy and industrial systems [3, 4]. Similarly, the 3.2 GHz band serves applications, like WiMAX networks, remote sensing, and mid-band 5G deployments, which provide a high-speed data transmission and an improved network capacity [5, 6]. The design of dual-band antennas often involves integrating slots into the antenna structure to achieve specific resonant characteristics. The slot dimensions and placements are critical for tailoring radiation patterns and ensuring optimal performance [7]. Reconfigurable antennas, incorporating diodes, enable the switching between operating frequencies by altering feeding points or tuning networks, further expanding operational flexibility [8].

The versatility and efficiency of dual-band antennas make them indispensable for modern communication systems. By supporting multiple frequency bands, they simplify the deployment of communication protocols, reduce the need for multiple single-band antennas, and optimize resource utilization. This approach lowers equipment, installation, and maintenance costs while enhancing performance, integration, and space efficiency [9, 10]. In addition to cost and compactness, dual-band antennas improve network reliability and coverage by minimizing interference and offering frequency diversity. These features are particularly valuable in wireless communication and radio frequency systems, where the space, cost, and performance constraints are paramount [11]. Achieving optimal dual-band performance requires selecting the appropriate frequency bands, antenna types (e.g., patch, slot, or dipole), and carefully designing matching networks and isolation techniques, particularly in complex systems like MIMO [12-14]. Key parameters, such as gain, radiation efficiency, and bandwidth, must be evaluated to ensure that the antenna meets performance requirements for both frequency bands [15]. Simulation tools, like CST and HFSS, are invaluable for modeling antenna designs and

predicting performance metrics. These tools enable iterative adjustments and optimization before moving to physical prototyping [16]. By addressing critical factors, such as frequency bands, impedance matching, isolation, gain, efficiency, and radiation patterns, designers can achieve highly optimized dual-band antenna systems [17].

II. ANTENNA DESIGN

For wideband operation, circular patch antennas are commonly designed as multiband antennas. The specific design depends on factors, such as the application, available space, and the preferred frequency bands, as illustrated in Figure 1.

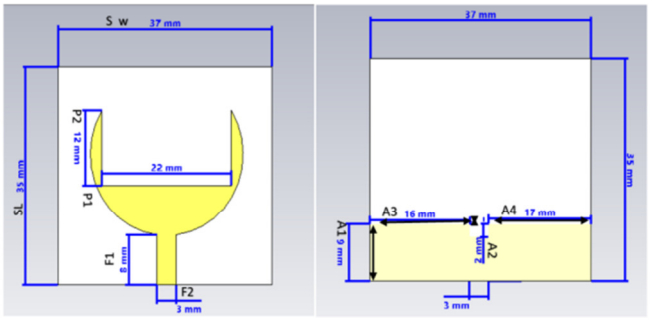

Fig. 1. Circular patch antenna design.

A. Design Steps

Optimizing bandwidth is crucial to maximizing the performance of dual-band antennas. The key techniques and considerations involved are provided below:

- Substrate Thickness

Increasing the substrate thickness broadens impedance matching, enhancing bandwidth. This approach is particularly effective when combined with advanced feeding techniques.

- Feeding Techniques

Aperture-coupled feeding, where the patch is fed through an aperture in the ground plane, provides better isolation between the feed and the radiating element, resulting in a wider bandwidth.

- Slot Length Optimization

Adjusting the lengths of stubs or slots shifts resonant frequencies and improves bandwidth. This technique allows fine-tuning to meet specific performance targets.

- Circular Patch Radius

Optimizing the radius of the circular patch is essential to achieve resonance at the desired frequencies. The radius directly affects both the resonant frequency and the bandwidth of the patch antenna.

By applying these techniques, the design can meet the stringent demands of the modern communication systems while achieving efficient dual-band operation.

B. Formulas and Parameters

The design of circular patch antennas relies on specific formulas to calculate dimensions and performance characteristics:

- Radius of Circular Patch

$$a = \frac{F}{\sqrt{1+\frac{2h}{\pi \cdot \varepsilon_r \cdot F \cdot \left[ln\left(\frac{F \cdot \pi}{2h}\right)+1.7726\right]}}} \quad (1)$$

- Effective Dielectric Constant (F)

$$F = \frac{8.791 \times 10^9}{f_r \cdot \sqrt{\varepsilon_r}} \quad (2)$$

Where h is the height of the substrate, ε_r is the dielectric constant of the substrate, and f_r is the resonant frequency.

- Wavelength Calculation

The wavelength (λ) is inversely proportional to the frequency (f), calculated as:

$$\lambda = \frac{c}{f} \quad (3)$$

where f is the frequency of the band and c is the speed of light [18].

III. RESULTS

The antenna's performance was evaluated using the -10 dB reflection coefficient criterion, which indicates that only 1% of the power is reflected. At the resonant frequencies of 3.7 GHz and 6.2 GHz, the reflection coefficients were -30 dB and -32 dB, respectively, as displayed in Figure 2. The Voltage Standing Wave Ratio (VSWR), a measure of reflected power, was within the acceptable range of 1 to 2 for dual-band operation, with the ideal value being 1, as depicted in Figure 3.

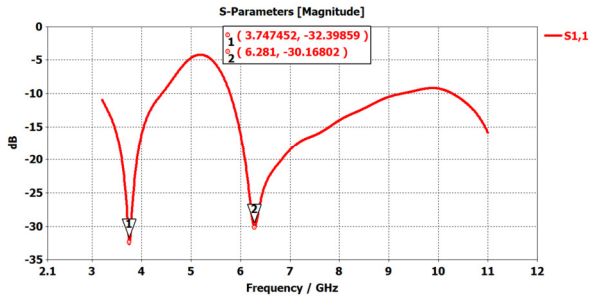

Fig. 2. Reflection coefficient (S_{11}) versus frequency.

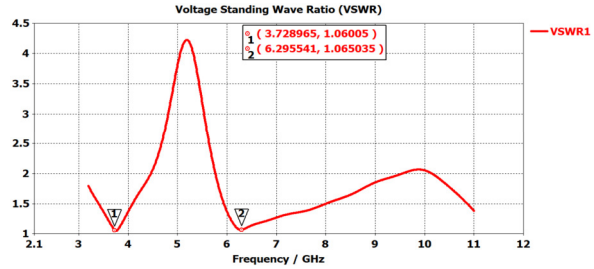

Fig. 3. VSWR curve across different frequencies.

The input impedance, defined as the ratio of voltage to current, (or the electric to magnetic field ratio) at the antenna input, showed that the real part of the impedance matched 50 ohms, while the imaginary part was near zero, indicating proper impedance matching, as portrayed in Figures 4(a) and 4(b).

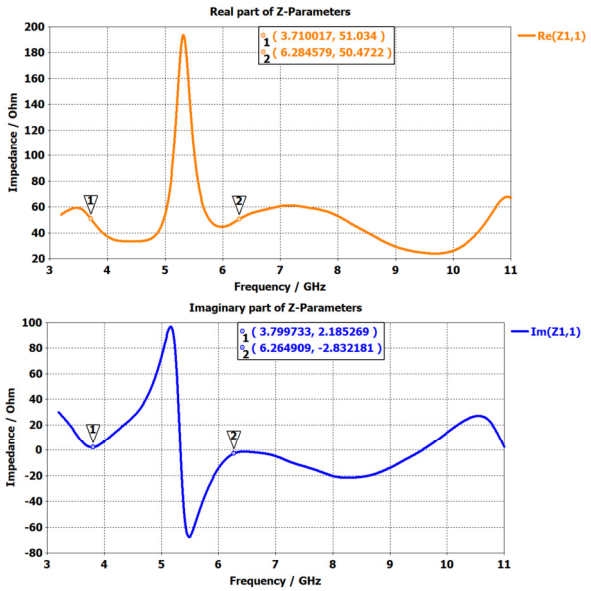

Fig. 4. The input impentance: (a) real part and (b) imaginary part.

The antenna achieved a maximum gain of 3.5 dB, with a directivity of 4.5 dB, as observed in Figures 5 and 6, and demonstrated high efficiency at 86%, as can be seen in Figure 7.

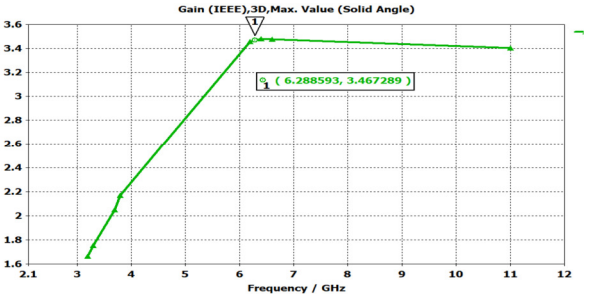

Fig. 5. Maximum gain versus frequency plot.

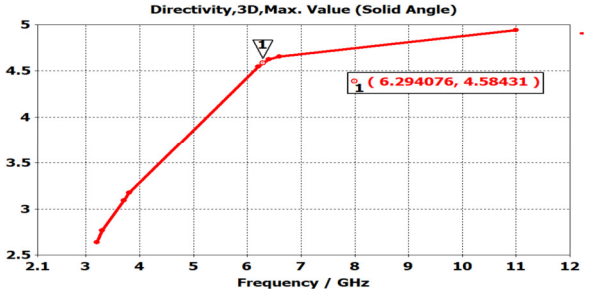

Fig. 6. Directivity versus frequency plot.

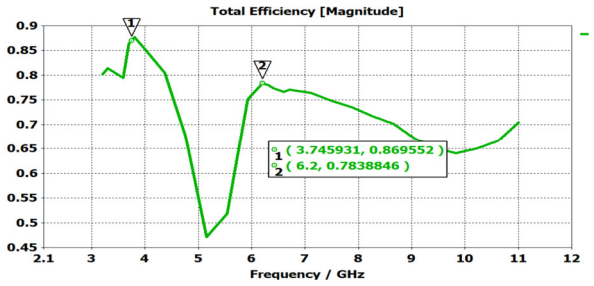

Fig. 7. Total efficiency versus frequency plot.

The surface current distribution analysis revealed a maximum current of 2.95 A/m at 6.2 GHz and 2.9 A/m at 3.7 GHz, as presented in Figures 8(a) and 8(b).

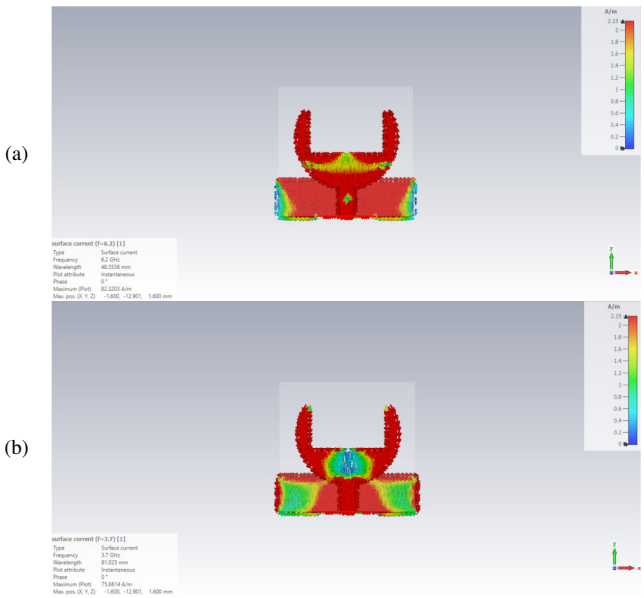

Fig. 8. Surface current at (a) 6.3 GHz and (b) 3.7 GHz.

The E-field and H-field distributions were observed at both frequencies, as evidenced in Figures 9 and 10, and the far-field radiation patterns confirmed a stable operation at 3.7 GHz and 6.2 GHz, as exhibited in Figure 11. Additionally, the wavelengths of the antenna were calculated as 0.081 m at 3.7 GHz and 0.048 m at 6.2 GHz, further validating its dual-band performance. The key design parameters of the antenna, including substrate dimensions, patch dimensions, feed line dimensions, and material properties, are summarized in Table I. These parameters were carefully chosen to optimize the antenna's performance, such as impedance matching, bandwidth, and radiation efficiency. A comparison of the proposed antenna design with previously reported designs is presented in Table II, where key metrics, such as dimensions, efficiency, directivity, maximum gain, and dual-band operational frequencies, are illustrated. The proposed antenna demonstrates superior performance, achieving an efficiency of 86%, a directivity of 4.5, and dual-band operation at 3.7 GHz and 6.2 GHz, with compact dimensions of 37 × 35 mm, outperforming many of the existing designs in terms of bandwidth and efficiency.

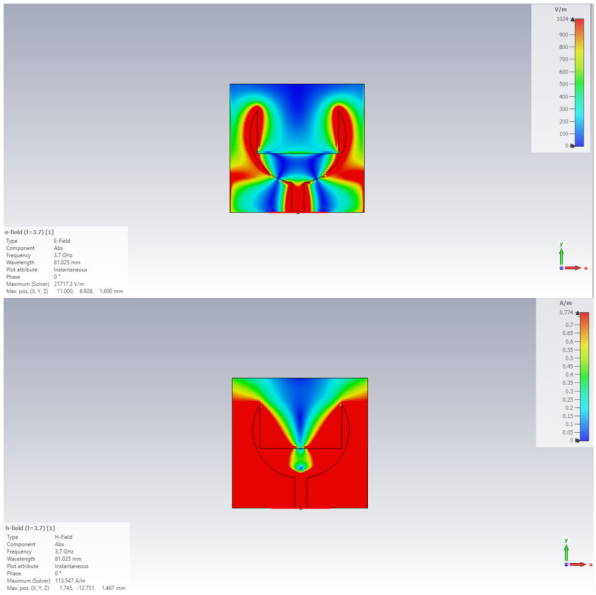

Fig. 9. (a) E-field and (b) H-field at 3.7 GHz.

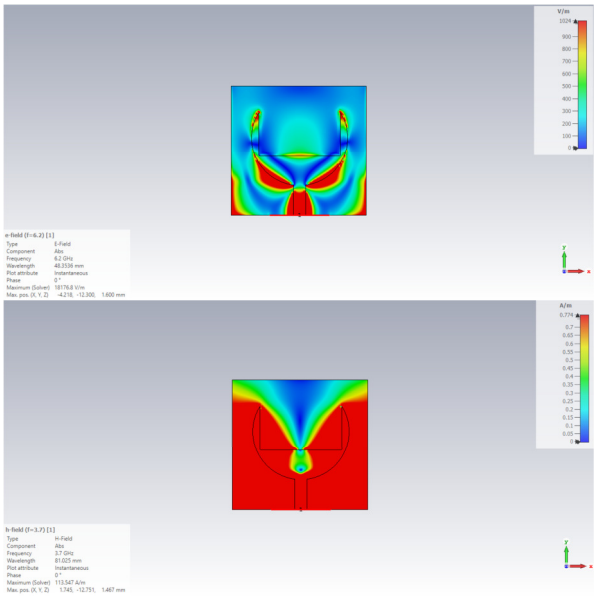

Fig. 10. (a) E-field and (b) H-field at 6.2 GHz.

TABLE I. ANTENNA PARAMETERS

Parameter	Value	Parameter	Value
SW	37 mm	*A1*	9 mm
SL	35 mm	*A2*	2 mm
P1	22 mm	*A3*	16 mm
P2	12 mm	*A4*	17 mm
F1	8 mm	ε_r	4.3
F2	3 mm	*h*	1.6

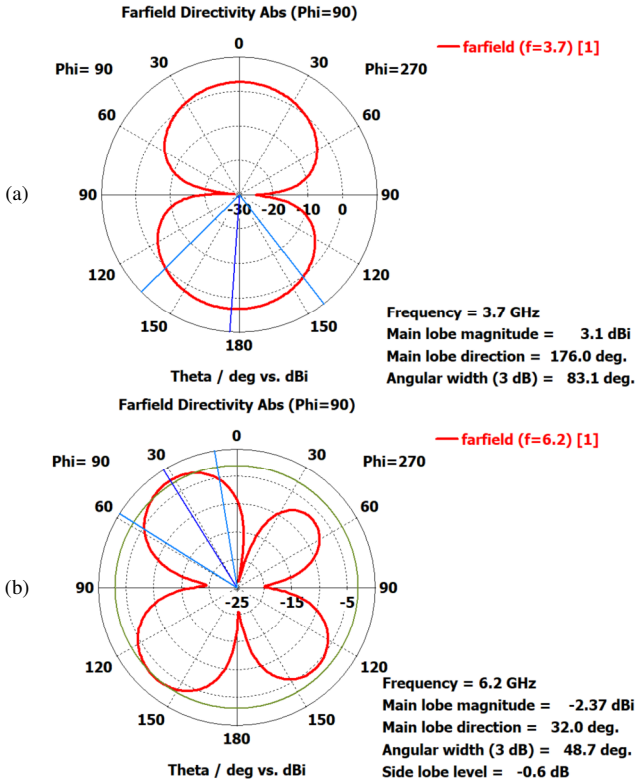

Fig. 11. H-field at (a) 3.7 GHz and (b) 6.2 GHz.

TABLE II. COMPARISON OF THE PROPOSED ANTENNA DESIGN WITH OTHER STUDIES

Ref.	Dimensions (mm)	yield (%)	Directivity	Max Gain (dBi)	Dual Bandwitch (GHz)
[19]	12×12	78	3.48	4.3	3.2, 3.7
[20]	13×19	75	3.8	3.1	2.4
[21]	38×38	98	3.56	2.4	2.4
[22]	35×40	83	4.23	2.89	1.24
[23]	38×25	80	4.14	2.85	3.6
[24]	25×25	70	4	3.4	7.85
[25]	50×50	79	3.2	2.053	2.4, 5.5
Proposed	37×35	86	4.5	3.47	3.7,6.2

IV. CONCLUSION

A miniaturized dual-band implantable antenna is presented for mobile application services as well as industrial and scientific applications. Compared to traditional dual-band antennas, the proposed design achieves significant improvements in performance while maintaining compact dimensions of 37 × 35 × 1.6 mm³. The antenna operates efficiently at dual frequencies of 3.7 GHz and 6.2 GHz, demonstrating stable radiation patterns, consistent gain, and high efficiency, which are crucial for modern communication systems, including 5G and other high-frequency applications. The innovative design incorporates a circular metal patch with rectangular-shaped slots, enabling broadband impedance matching and enhanced performance. The proposed antenna achieves a gain of 3.47 dBi, a directivity of 4.5, and an efficiency of 86%. When compared to previous works, it

demonstrates superior performance in terms of efficiency and bandwidth while maintaining a compact size. For instance, while authors in [19] reported an efficiency of 78% and dual-band operation at 3.2 GHz and 3.7 GHz with dimensions of 12 × 12 mm², the proposed antenna offers higher efficiency and wider dual-band coverage. Similarly, when compared to [21] and [25], where efficiencies of 98% and 79% were, respectively, reported, the proposed design strikes a balance between compactness, efficiency, and gain. Overall, this dual-band antenna offers a competitive advantage, meeting the increased data demands and diverse frequency requirements of modern mobile systems while ensuring seamless integration into devices.

V. FUTURE TRENDS

Future trends in wireless communication are indeed moving towards dual-band and multi-band designs to address interference issues, improve gain, and enhance the directivity of multi-band networks. Future wireless networks are expected to transition from single band to Multi-Band Networks (MBNs), where various frequency bands coexist. This helps manage the exponential growth of data traffic and meet the massive connectivity requirements. Advanced antenna technologies, like massive Multiple-Input Multiple-Output (MIMO) and metamaterial-based antennas, are being developed to improve performance. Moreover, dual-band, and multi-band designs reduce interference by allowing devices to switch between different frequency bands based on the network conditions. These advancements are paving the way for more robust and efficient wireless communication systems, especially as we move towards 6G and beyond.

REFERENCES

[1] Y. Zhai *et al.*, "Recent Advances on Dual-Band Electrochromic Materials and Devices," *Advanced Functional Materials*, vol. 32, no. 17, 2022, Art. no. 2109848, https://doi.org/10.1002/adfm.202109848.

[2] X. Fan *et al.*, "Photonic-assisted multi-format dual-band microwave signal generator without background noise," *Optics Express*, vol. 31, no. 11, pp. 18346–18355, May 2023, https://doi.org/10.1364/OE.488780.

[3] M. Gao, Y. He, J. Nan, Z. Yang, and C. Wang, "A miniaturized ultra-wideband filter with high rejection and selectivity based on dual-notch bands," *PLOS ONE*, vol. 19, no. 8, Jul. 2024, Art. no. e0306730, https://doi.org/10.1371/journal.pone.0306730.

[4] Q. Liu, H. Liu, W. He, and S. He, "A Low-Profile Dual-Band Dual-Polarized Antenna With an AMC Reflector for 5G Communications," *IEEE Access*, vol. 8, pp. 24072–24080, Jan. 2020, https://doi.org/10.1109/ACCESS.2020.2970473.

[5] K. N. Paracha *et al.*, "A Low Profile, Dual-band, Dual Polarized Antenna for Indoor/Outdoor Wearable Application," *IEEE Access*, vol. 7, pp. 33277–33288, Jan. 2019, https://doi.org/10.1109/ACCESS.2019.2894330.

[6] C. Shi, J. Zou, J. Gao, and C. Liu, "Gain Enhancement of a Dual-Band Antenna with the FSS," *Electronics*, vol. 11, no. 18, Jan. 2022, Art. no. 2882, https://doi.org/10.3390/electronics11182882.

[7] S. Chandravanshi, K. K. Katare, and M. J. Akhtar, "A Flexible Dual-Band Rectenna With Full Azimuth Coverage," *IEEE Access*, vol. 9, pp. 27476–27484, Jan. 2021, https://doi.org/10.1109/ACCESS.2021.3058239.

[8] S. Zhao *et al.*, "Dual-band electrochromic materials for energy-saving smart windows," *Carbon Neutralization*, vol. 2, no. 1, pp. 4–27, 2023, https://doi.org/10.1002/cnl2.38.

[9] R. Joshi *et al.*, "Dual-Band, Dual-Sense Textile Antenna With AMC Backing for Localization Using GPS and WBAN/WLAN," *IEEE Access*, vol. 8, pp. 89468–89478, Jan. 2020, https://doi.org/10.1109/ACCESS.2020.2993371.

[10] Q. Huang *et al.*, "A dual-band transceiver with excellent heat insulation property for microwave absorption and low infrared emissivity compatibility," *Chemical Engineering Journal*, vol. 446, Oct. 2022, Art. no. 137279, https://doi.org/10.1016/j.cej.2022.137279.

[11] X.-L. Yang, X.-W. Zhu, and X. Wang, "Dual-Band Substrate Integrated Waveguide Filters Based on Multi-Mode Resonator Overlapping Mode Control," *IEEE Transactions on Circuits and Systems II: Express Briefs*, vol. 70, no. 6, pp. 1971–1975, Jun. 2023, https://doi.org/10.1109/TCSII.2023.3236365.

[12] F. Liu, J. Guo, L. Zhao, G.-L. Huang, Y. Li, and Y. Yin, "Dual-Band Metasurface-Based Decoupling Method for Two Closely Packed Dual-Band Antennas," *IEEE Transactions on Antennas and Propagation*, vol. 68, no. 1, pp. 552–557, Jan. 2020, https://doi.org/10.1109/TAP.2019.2940316.

[13] T. Bai, W. Li, G. Fu, Q. Zhang, K. Zhou, and H. Wang, "Dual-band electrochromic smart windows towards building energy conservation," *Solar Energy Materials and Solar Cells*, vol. 256, Jul. 2023, Art. no. 112320, https://doi.org/10.1016/j.solmat.2023.112320.

[14] S. Costanzo, F. Venneri, A. Borgia, and G. D. Massa, "Dual-Band Dual-Linear Polarization Reflectarray for mmWaves/5G Applications," *IEEE Access*, vol. 8, pp. 78183–78192, Jan. 2020, https://doi.org/10.1109/ACCESS.2020.2989581.

[15] S. Anwar, "Dual-band detection based on metamaterial sensor at terahertz frequency," *Optical Review*, vol. 30, no. 3, pp. 300–309, Jun. 2023, https://doi.org/10.1007/s10043-023-00808-w.

[16] X. Y. Zhang, J.-X. Chen, Q. Xue, and S.-M. Li, "Dual-Band Bandpass Filters Using Stub-Loaded Resonators," *IEEE Microwave and Wireless Components Letters*, vol. 17, no. 8, pp. 583–585, Dec. 2007, https://doi.org/10.1109/LMWC.2007.901768.

[17] X. Zheng, Y. Pan, and T. Jiang, "UWB Bandpass Filter with Dual Notched Bands Using T-Shaped Resonator and L-Shaped Defected Microstrip Structure," *Micromachines*, vol. 9, no. 6, Jun. 2018, Art. no. 280, https://doi.org/10.3390/mi9060280.

[18] M. S. L. Gade, G. N. Prasad, A. Gantala, P. Anjaneyulu, and H. A. Shaik, "Design of circular microstrip patch antenna and its simulation results," *Journal of Advanced Research in Dynamical and Control Systems*, vol. 9, no. 4, pp. 230–239, Oct. 2017.

[19] S. R. Agilesh, B. T. P. Madhav, A. Gangadhar, and S. S. Chintalapati, "Design of Dual Band Substrate Integrated Waveguide (SIW) Antenna with Modified Slot for Ka-Band Applications," *Engineering, Technology & Applied Science Research*, vol. 14, no. 4, pp. 14923–14928, Aug. 2024, https://doi.org/10.48084/etasr.7620.

[20] M. J. Hakeem and M. M. Nahas, "Improving the Performance of a Microstrip Antenna by Adding a Slot into Different Patch Designs," *Engineering, Technology & Applied Science Research*, vol. 11, no. 4, pp. 7469–7476, Aug. 2021, https://doi.org/10.48084/etasr.4280.

[21] S. Nelaturi and N. V. S. N. Sarma, "Compact Wideband Microstrip Patch Antenna based on High Impedance Surface," *Engineering, Technology & Applied Science Research*, vol. 8, no. 4, pp. 3149–3152, Aug. 2018, https://doi.org/10.48084/etasr.1971.

[22] J. R. Panda and R. S. Kshetrimayum, "An F-shaped printed monopole antenna for dual-band RFID and WLAN applications," *Microwave and Optical Technology Letters*, vol. 53, no. 7, pp. 1478–1481, 2011, https://doi.org/10.1002/mop.26060.

[23] A. K. Gautam, A. Bisht, and B. K. Kanaujia, "A wideband antenna with defected ground plane for WLAN/WiMAX applications," *AEU - International Journal of Electronics and Communications*, vol. 70, no. 3, pp. 354–358, Mar. 2016, https://doi.org/10.1016/j.aeue.2015.12.013.

[24] H. Fallahi and Z. Atlasbaf, "Bandwidth enhancement of a CPW-fed monopole antenna with small fractal elements," *AEU - International Journal of Electronics and Communications*, vol. 69, no. 2, pp. 590–595, Feb. 2015, https://doi.org/10.1016/j.aeue.2014.11.011.

[25] M. Mabaso and P. Kumar, "A dual band patch antenna for Bluetooth and wireless local area networks applications," *International Journal of Microwave and Optical Technology*, vol. 13, no. 5, pp. 393–400, Sep. 2018, https://doi.org/10.6084/m9.figshare.20000165.